

A dynamic fatigue study of soda–lime silicate and borosilicate glasses using small scale indentation flaws

T. P. Dabbs, B. R. Lawn* & P. L. Kelly

Department of Applied Physics, School of Physics, University of New South Wales, Kensington, N.S.W. 2033, Australia

Manuscript received 27 July 1981

The dynamic fatigue characteristics of two glasses, soda–lime silicate and borosilicate, in water have been studied using a controlled indentation flaw technique. It is argued that the indentation approach offers several advantages over more conventional fatigue testing procedures: (i) the reproducibility of data is relatively high, eliminating statistics as a basis of analysis; (ii) the flaw ultimately responsible for failure is well defined and may be conveniently characterised before and after (and during, if necessary) the strength test; (iii) via adjustment of the indentation load, the size of the flaw can be suitably predetermined. Particular attention is devoted to the third point because of the facility it provides for systematic investigation of the range of flaw sizes over which macroscopic crack behaviour remains applicable.

The first part of the paper summarises the essential fracture mechanics theory of the extension of an indentation flaw to failure. A distinctive feature of this theory is the explicit incorporation of a residual contact term associated with elastic/plastic mismatch stresses in the indentation processes into the stress intensity factor for the growing crack. A scheme is thus devised whereby the indentation load is treated as a key test variable in the construction of universal dynamic fatigue curves. It is demonstrated that basic kinetic fracture parameters, relating to the crack velocity functions for macroscopic cracks, may be obtained in the usual way from slope and intercept measurements on plots of strength against stress rate; accommodation of the residual stress term is achieved via simple 'transformation' relations for converting 'apparent' kinetic parameters (i.e. evaluated on the basis of a flaw with no residual stress) to 'true' values.

In the next part of the paper the results of dynamic fatigue tests on glass rods in distilled water are described. Data are obtained for Vickers indentation loads in the range 0.05–100 N, corresponding to contact dimensions of 2–100 μm . The data fall on universal fatigue curves, within experimental scatter, as predicted. Evaluations of kinetic fracture parameters from these curves are consistent with those from independent de-

terminations by other workers using macroscopic crack configurations.

Finally, the implications of the results in relation to the response of 'natural' flaws are discussed. It is suggested that flaws in the sub-micrometre domain could be of a nature somewhat different to that of true microcracks. Larger flaws, in the size range covered here, appear to behave as macroscopic cracks, provided account is taken of the crack driving force associated with residual stress fields. The residual term is shown to have a vital influence on the mechanics to failure; ignoring this term can lead to serious errors in evaluations of the parameters from fatigue data. This influence is manifest in borosilicate as well as soda–lime glass, even though the former is 'anomalous' in its indentation deformation properties, with significantly reduced susceptibility to elastic/plastic mismatch processes.

Numerous recent studies have provided compelling evidence that fracture mechanics data on macroscopic cracks can be used to predict the fatigue properties of glasses and other ceramics.^(1–7) The underlying basis of the fracture mechanics approach is that fatigue failure occurs from rate dependent, subcritical extension of a microscopic flaw to an instability configuration; it is implied that the flaw is simply a scaled down version of the well defined macrocrack. Analysis of the strength characteristics under fatigue conditions then follows from two basic starting equations for the crack propagation: the first equation represents the driving force on the crack, $K \sim \sigma c^{1/2}$, where K is a stress intensity factor, σ is a uniform applied tensile stress, and c is a characteristic crack dimension; the second equation represents the ensuing stress enhanced motion of the crack, $v = v(K)$, where $v(K)$ is a crack velocity function. In principle, once the parameters of these two equations have been determined from controlled fracture specimens, the foundation is laid for the analytical prediction of fatigue response over a seemingly unlimited range of service conditions.

However, the fracture mechanics approach to the fatigue problem is not without its difficulties. For a

*Now at Fracture and Deformation Division, National Bureau of Standards, Washington, DC 20234, USA.

start, there is the statistical aspect of strength properties. Strength measures a combination of intrinsic toughness and flaw size, and the latter quantity is subject to considerable variability in the typical brittle material. It is accordingly necessary to test large sample populations to obtain reliable parameters for prediction purposes. Some attempts have been made to circumvent this difficulty by introducing controlled abrasion flaws into the test surfaces.⁽⁸⁾ This procedure, although improving the reproducibility of results, nevertheless does not allow for *a priori* characterisation of the critical flaw; apart from the problem of quantifying the growth history of any individual abrasion flaw, it is generally not possible to specify which flaw will ultimately cause the failure.

A second difficulty concerns the assumed forms of the starting fracture mechanics equations mentioned above. The crack velocity function $v(K)$ has been subjected to particular scrutiny in this regard. It is common for this function to show more than one distinctive region of behaviour, corresponding to changes in rate controlling mechanism in a given material/environment system, although there is some doubt as to whether this is likely to be of significant influence in fatigue behaviour;^(3, 9) the region of lowest velocities (region I), governed by reaction kinetics at the crack tip, is expected to be dominant in the determinations of times to failure. On the other hand, knowledge of the exact analytical form of the velocity function in this region is vitally important when extrapolating short term data to the long lifetime domain;⁽¹⁰⁾ in this context it needs to be noted that the $v(K)$ equations in general use are empirically based. But it is not only the crack velocity function which requires qualification. The simplistic relation $K \sim \sigma c^{1/2}$ must be seen as a special case (the 'Griffith limit') of a more general configuration where the forces initially responsible for creating the flaw persist (in whole or in part) to augment the ensuing crack propagation force.⁽¹¹⁾ Studies of indentation induced cracks in glass in these laboratories^(12, 13) have provided a convenient model 'flaw' system for quantifying residual stress effects of this kind. A sharp contact geometry is used to create a highly localised region of irreversible deformation, from which the cracks generate. It then becomes necessary to add an appropriate residual term to the stress intensity factor for crack propagation to allow for elastic/plastic mismatch contributions to the fracture driving force.⁽¹⁴⁾ If ignored in fatigue analyses, the residual term can lead to large discrepancies between predicted and observed strength characteristics.^(15, 16)

A third difficulty with the fracture mechanics approach relates to the scale of the flaw. Do the laws of macroscopic crack growth continue to apply at the level of the typical flaw? There is now some evidence, particularly from studies on ultra high strength optical fibres,^(17, 18) to suggest that the entire nature of flaws in glass changes as the scale is reduced below some critical level. This is consistent with the concept of a threshold for development of well defined microcracks in concentrated stress fields,⁽¹⁹⁾ a concept fully borne out by analysis of indentation flaw initiation in a wide

range of brittle materials.^(20, 21) Extrapolation into the ultra high strength domain is therefore subject to an element of uncertainty, requiring that due attention be paid to potentially significant departures from the conventional mechanics of fatigue failure.

The present paper describes a study of the dynamic fatigue characteristics of the glass/water system, using the indentation flaw technique as a means of circumventing the major difficulties just described. Indentation patterns are generally highly reproducible, in which case the statistical element of strength measurement is conveniently eliminated, thereby allowing for accurate evaluation of materials. Moreover, the failure site is identified beforehand, so one may follow the crack evolution throughout the test sequence. With this facility, it is possible to investigate the factors which contribute to the basic fracture mechanics equations; the important contribution of residual stress effects to the stress intensity factor is a case in point which has already been mentioned. Finally, since the scale of the indentation event is readily amenable to strict control via the contact load, the way is open for establishing the range of validity of macroscopic crack laws. This last point forms one of the major thrusts of the work to be described below. In this sense our study may be seen as an extension of earlier indentation fatigue analyses of the glass/water system.^(15, 16) However, a somewhat simplified experimental procedure, based on a more recently developed theoretical description,⁽²²⁾ is adopted here. Further, in addition to the soda-lime glass type used previously, a borosilicate glass is also analysed. Apart from providing a wider base for comparison with results from other workers,⁽²³⁻²⁵⁾ the latter glass type, which is 'anomalous' in the indentation deformation response,⁽²⁶⁾ affords the opportunity for investigating a material somewhat removed from the idealised stereo-type assumed in the theoretical derivations.

Theoretical background

Vickers induced radial crack system as strength controlling flaw

We summarise here the essential features of the general theory of dynamic fatigue for indentation flaws,⁽²²⁾ with additional attention to the role of the scale of contact, as determined by the indentation load, as a test variable. Simplicity in the experimental test programme and in the ensuing analysis of the data is a key consideration in the formulation of the problem. To facilitate this simplicity, it is necessary to incorporate some ostensibly complicating elements into the mathematical derivations, notably a residual contact term.

A schematic of the model indentation flaw system is shown in Figure 1.⁽²¹⁾ The pattern corresponds to that produced by a standard Vickers diamond pyramid indenter used in routine hardness testing. At a peak load, P , the pattern has characteristic surface dimensions, a_0 representing a central ('plastic') deformation zone and c_0 representing the radial traces of as-

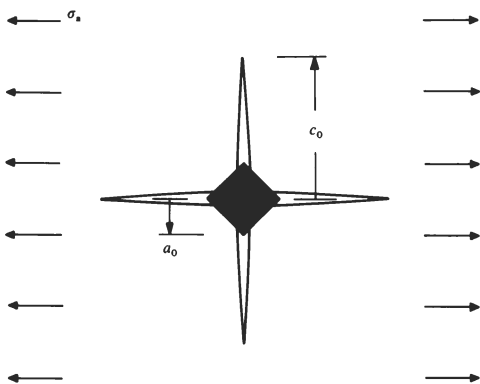


Figure 1. Schematic surface view of deformation/fracture pattern produced by a Vickers indenter showing the characteristic radial crack dimension, c_0 , the hardness impression dimension, a_0 , and the subsequent applied tensile stress, σ_a . The driving force for radial crack system determined by peak indentation load, P , is not indicated.

sociated cracks. The dimension a_0 is a measure of the resistance to irreversible deformation, and relates to P via the material hardness, H , defined as the mean contact pressure, by

$$a_0 = (P/2H)^{1/2}. \quad (1)$$

Similarly, the dimension c_0 is a measure of the resistance to crack propagation and relates to P via the material toughness, K_c , the critical stress intensity factor for crack extension under conditions of mechanical equilibrium, by

$$c_0 = (\chi_r P / K_c)^{2/3} \quad (2)$$

where χ_r is a geometrical (material dependent⁽¹⁴⁾) parameter. Comparison of the dimensions in Equations (1) and (2) affords a useful measure of material 'brittleness',⁽²¹⁾ the region $c_0 \lesssim a_0$ is of particular interest in the context of the present work, for it signifies that the flaw must be encompassed within the deformation zone, corresponding to the sub-threshold realm of crack initiation. The effect of the deformation zone on the crack development is not confined to this region, however; it is found that well developed radial cracks in glass, i.e. at $c_0 \gg a_0$, remain well within the sphere of influence of the residual stress field (as revealed by birefringence⁽¹³⁾) centred about the contact area. In fact, the residual stress component of the indentation field is the source of the primary crack extension force, causing the radial crack to grow to its equilibrium size, c_0 , during the unloading half cycle.⁽¹⁴⁾ An important manifestation of this residual stress component is the continued, slow crack growth that is observed in glass after completion of the contact cycle;⁽¹³⁾ this growth, activated by atmospheric moisture, takes the crack to some non-equilibrium configuration, say, $c'_0 > c_0$.

Consider now the response of the radial crack flaw at c'_0 to a subsequently applied uniform tensile stress σ_a . The stress intensity factor for the crack must now contain two components^(12, 13)

$$K = \chi_r P / c^{3/2} + \sigma_a (\pi \Omega c)^{1/2} \quad (c \geq c'_0) \quad (3)$$

where Ω is another geometrical parameter. We may

note that Equation (2) follows from Equation (3) if we insert the equilibrium requirements $K = K_c$ and $c'_0 = c_0$ at the initial condition $\sigma_a = 0$. Also, at zero residual stress, $\chi_r = 0$, Equation (3) reduces to the special case of Griffith-like cracks. The strength is then determined as the level of applied stress, $\sigma_a = \sigma$, at which a configuration of unstable equilibrium is attained, i.e. at which the conditions $K = K_c$ and $dK/dc > 0$, are satisfied.

Inert strength

In any analysis of fatigue it is convenient to take the inert strength as a reference baseline. This is the strength that obtains in a truly inert environment such that no nonequilibrium crack extension occurs during stressing to failure; inert strengths may be effectively achieved by testing at fast load rates or at low temperatures. Accordingly, putting $K = K_c$ into Equation (3) and solving for the applied stress,⁽¹³⁾

$$\sigma_a = [K_c / (\pi \Omega c)^{1/2}] [1 - \chi_r P / K_c c^{3/2}], \quad (4)$$

we may identify the inert strength $\sigma = \sigma_i = \sigma_m$ in terms of a maximum in the function $\sigma_a(c)$, corresponding to an instability in the function $K(c)$ in Equation (3), at (σ_m, c_m) , where

$$c_m / P^{2/3} = 4^{2/3} [\chi_r / K_c]^{2/3} \quad (5a)$$

$$\sigma_m P^{1/3} = (3/4^{4/3}) [K_c / (\pi \Omega)^{1/2}] [K_c / \chi_r]^{1/3}. \quad (5b)$$

Physically, the presence of the maximum means that the crack will undergo a stage of precursor stable growth, from c'_0 to c_m , prior to failure. As a corollary to this point, the condition $c'_0 < c_m$ is a necessary proviso for identifying σ_i with σ_m . It may be noted that the critical configuration expressed by Equation (5) is totally independent of c'_0 so that, within the confines of the proviso just mentioned, the inert strength is insensitive to the crack history between indentation and failure testing.

In this way σ_m and c_m serve as useful reference parameters for indentation flaws produced at any given load, P .⁽²²⁾ In our present case, where P is to be used as an important test variable, it may be seen from Equation (5) that the constant quantities $c_m / P^{2/3}$ and $\sigma_m P^{1/3}$ afford a more general basis for data reduction.

Dynamic fatigue strength

Let us now deal with the strength behaviour under dynamic fatigue conditions, i.e. stressing at a fixed rate, $\sigma_a = \dot{\sigma}_a t$ ($\dot{\sigma}_a$ constant), such that nonequilibrium crack extension occurs prior to failure. For glass, such nonequilibrium extension occurs because of the accessibility of the crack tip to moisture. Thus the approach to the final crack instability proceeds along some subcritical path, $K(c) < K_c$, in accordance with some specified crack velocity function, until Equation (4) is ultimately satisfied at $c = c_f > c_m$; the corresponding strength region $\sigma < \sigma_m$ appropriately defines the domain of dynamic fatigue. If we adopt as representative over the entire subcritical region, $0 < K < K_c$, the most commonly used crack velocity

function⁽¹⁰⁾

$$v = v_0(K/K_c)^n \tag{6}$$

where v_0 and n are kinetic constants for the given material/environment system, we obtain from Equation (1) the differential equation⁽¹⁵⁾

$$\dot{c}/v_0 = \{[\chi_r/K_c]P/c^{3/2} + [(\pi\Omega)^{1/2}/K_c]\dot{\sigma}_a c^{1/2}t\}^n \tag{7}$$

This must generally be solved numerically for the time to failure, t_f , i.e. the time to take the crack from c'_0 to c_f , for any given values of P and $\dot{\sigma}_a$; the strength $\sigma = \dot{\sigma}_a t_f$ then follows.

At this point it is useful to rewrite Equation (7) in terms of reduced variables and so avoid having to specify numerous adjustable quantities for integration to proceed. The reference parameters σ_m and c_m defined in the previous section are used as the basis for normalisation, thus:⁽²²⁾

$$S_a = \sigma_a/\sigma_m \tag{8a}$$

$$C \equiv c/c_m \tag{8b}$$

$$T \equiv tv_0/c_m \tag{8c}$$

Equation (7) accordingly reduces to

$$\dot{C} = (1/4C^{3/2} + 3\dot{S}_a C^{1/2} T/4)^n \tag{9}$$

where $\dot{C} = dC/dT$ and $\dot{S}_a = S_a/T$. Strictly, the time to failure T_f should be evaluated in terms of an initial crack size, C'_0 , and final crack size, C_f (>1 , as determined by the condition $\dot{C} = 1$). However, it can be shown that the integration is insensitive to the initial crack size in the range $C_0 \leq C'_0 \leq C_m$, where $C_0 = 0.397$, cf. Equations (2) and (5a), and $C_m = 1$.⁽²²⁾ Under such circumstances one may take $T = 0$ and $C = 0.397$ as an invariant initial condition. It will be noted that Equation (9) contains no reduced variable corresponding to χ_r in Equation (7); the residual stress term has conveniently been incorporated into the reference crack dimension, c_m , in Equation (5a).

Thus for any fixed value of the kinetic constant, n , Equation (9) may be solved to generate the dynamic fatigue function, $S(S_a)$.⁽²²⁾ When plotted in logarithmic coordinates these functions tend to linearity in the fatigue domain $S < S_i = 1$ (this tendency increasing with n), and may accordingly be represented by the usual kind of strength/stress rate relation⁽²⁻⁷⁾

$$S = (\Lambda' \dot{S}_a)^{1/(n'+1)} \tag{10}$$

where Λ' and n' are intercept and slope parameters; the primed notation is used here to remind us that we are dealing with solutions of the fatigue equations with the residual stress term included, so data analysis from as-indented specimens using Equation (10) in the conventional manner would yield 'apparent' values for the constants in the crack velocity function. Both Λ' and n' can be uniquely related to the 'true' crack velocity exponent, n , by means of empirical analysis of the numerical fits to Equation (10);⁽²²⁾

$$n' = 0.763 n \tag{11a}$$

$$\Lambda' = 2.51 n^{0.462} \tag{11b}$$

Evaluation of fracture parameters from universal dynamic fatigue curves

Equation (10) lays the foundation for plotting dynamic fatigue data on universal curves, from which the true kinetic fracture constants may be evaluated. Taking note of the way in which the load variable, P , is displayed in Equation (5), we may write the normalised strength and stress rate from Equation (8) in the form

$$S = \sigma/\sigma_m = \sigma P^{1/3}/[\sigma_m P^{1/3}] \tag{12a}$$

$$\dot{S}_a = \dot{\sigma}_a c_m/\sigma_m v_0 = \dot{\sigma}_a P[(c_m/P^{2/3})/(\sigma_m P^{1/3})v_0] \tag{12b}$$

where the terms in square brackets are invariants for a given system. Then Equation (10) may be de-normalised thus

$$\sigma P^{1/3} = (\lambda'_p \dot{\sigma}_a P)^{1/(n'+1)} \tag{13}$$

where

$$\lambda'_p = \Lambda'(\sigma_m P^{1/3})^{n'}(c_m/P^{2/3})/v_0 \tag{14}$$

Combination with Equation (11) then gives

$$n = 1.31 n' \tag{15a}$$

$$v_0 = 2.84 n'^{0.462}(\sigma_m P^{1/3})^{n'}(c_m/P^{2/3})/\lambda'_p \tag{15b}$$

It is estimated that Equation (15a) is accurate to $\approx 1\%$, and Equation (15b) to $\approx 10\%$, in the region $n > 10$ ⁽²²⁾ (which covers most brittle solids studied thus far).

Hence a complete characterisation of fatigue response may be obtained from a universal, linear plot of $\log(\sigma P^{1/3})$ against $\log(\dot{\sigma}_a P)$ over the load range of interest, together with appropriate inert strength determinations. The fracture parameters evaluated from such analysis may be expected to be representative of true macroscopic crack behaviour.

Experimental

Materials preparation and test procedure

Rod specimens of soda-lime silicate (wt% composition 69SiO₂, 13Na₂O, 4CaO, 1B₂O₃, 4Al₂O₃, 2K₂O, 4BaO, 2MgO, 1 other) and borosilicate (81SiO₂, 13B₂O₃, 4Na₂O + K₂O, 2Al₂O₃) glass* were cut from 5 mm diameter cane into 215 mm lengths. All the rods were annealed, the soda-lime at 520°C and the borosilicate at 610°C, for 24 h to remove any existing surface stresses. They were then etched in a solution of 10% HF/10% H₂SO₄ for 6 min to nullify any large handling flaws.

Each rod was indented midway along its length with a standard Vickers indenter. Special care was taken to align the indenting pyramid symmetrically with respect to the rod, such that the impression diagonals (Figure 1) were oriented perpendicular and parallel to the rod axis. All such indentations were made in air, at a constant 10 s contact duration, using microhardness testing equipment covering a working load range 0.05-100 N. A microscopic examination

*Schott-Ruhrglas, GMBH.

was made of all indentation sites to ascertain first, whether crack initiation had occurred and second, the nature of the ensuing crack pattern. In accordance with a previous study,⁽²⁶⁾ radial crack formation was much better defined in the soda-lime than in the borosilicate specimens, the latter being complicated by the incidence of spurious ring cracks and a tendency for the radials to grow outward from points on the impression perimeter away from the corners. Bearing in mind our stated aim in this study to investigate the range of validity of macroscopic crack laws, the criterion for accepting any given specimen for subsequent strength testing was that there should be a reasonably well developed radial crack trace closely parallel to a rod circumference (thereby ensuring the existence of a suitable dominant flaw nearly normal to the designated tensile axis of the rod). For both glass types the minimum loading at which such a configuration obtained was of order 1 N, but for soda-lime glass this threshold could be reduced dramatically, to <0.05 N, by immersing the newly indented surfaces in a solution of 1% HF/1% H₂SO₄ for ≈ 60 s; borosilicate remained immune to any such treatment. A more detailed description of this crack initiation process will be given elsewhere.⁽²⁷⁾

The specimens which passed the above 'acceptance' test were then broken in four-point bending, using apparatus constructed in accordance with ASTM specifications,⁽²⁸⁾ with an inner span of 20 mm and an outer span of 60 mm. A crosshead testing machine was used to deliver the bending force, which was monitored at slow stress rates ($\lesssim 100$ MPa s⁻¹) by a conventional strain gauge instrumented load cell and at fast rates ($\gtrsim 100$ MPa s⁻¹) by a piezoelectric cell. Both cells gave a linear load/time response at constant crosshead speed; the stress at failure and the stress rate were then evaluated from this response using simple beam theory. The practical range of stress rates available with our equipment was 0.1–2000 MPa s⁻¹. To ensure that the indentation flaws were always located at the maximum tensile surface in the bending rig, a metal flag was attached to the end of each rod prior to indentation; it was then a simple matter of maintaining the flag vertical during the two stages of testing. The average interval between indentation and bending was ≈ 1 h, during which time the cracks were exposed to air (except, of course, for those specimens exposed to the post-indentation etch treatment mentioned above). During the bend test the crack environment was controlled to meet the requirements of equilibrium and nonequilibrium extension: inert environments were obtained either by blowing dry nitrogen gas through a plastic sleeve encasing the rod or by covering the indentation sites with a drop of silicone oil; the noninert environment was similarly obtained by covering the indentations with a drop of distilled water. All broken specimens were examined to confirm that failure had occurred from the indentation flaw; a few specimens broke from other origins (more frequently at the lower indentation loads) and these were deleted from the results. The post-indentation examinations served also to ensure that

the crack dimensions at failure were sufficiently small, \lesssim one-tenth of the rod diameter, for specimen size and shape effects to be neglected.

Before conducting the test runs proper, a preliminary check was made on soda-lime glass to investigate the strength characteristics of specimens containing cracks induced by post-indentation etching. It could be argued that such cracks might tend to be blunt and thereby give rise to higher strengths than appropriate to cracks produced in air. Accordingly, specimens were indented at $P = 0.7$ N, at which load spontaneous crack 'pop-in' occurred in about one half of the cases; those apparently free from cracks were etched. Inert strengths were then measured for both groups, giving 136 ± 10 MPa (12 specimens) and 134 ± 10 MPa (16 specimens) respectively. Thus the crack severity is insensitive to the formation history.

Determination of inert strength parameters

Test runs were made in silicone oil and nitrogen gas environments to determine the inert strength parameters contained in Equation (5). In the case of the nitrogen tests the rods were prepared with three ostensibly identical indentations in their surfaces instead of the usual one, for reasons to be made clear below. To obtain the parameter in σ_m , the strengths were measured over a range of indentation loads and stress rates for both glasses. The results are shown in Figure 2, as a plot of $\sigma_i P^{1/3}$ against $\dot{\sigma}_a P$; this mode of graphical representation, based on the scheme for normalising fatigue curve coordinates in Equation (12), is useful for establishing the domain of truly inert strengths. The soda-lime rods do in fact show some tendency to fatigue at $\dot{\sigma}_a P \lesssim 100$ MPa s⁻¹ N, indicating that the environments are not entirely free of moisture. The data points in Figure 2 represent means and standard deviations, in logarithmic coordinates, of 6–15 specimens. The average standard deviation is $\approx 8\%$, somewhat higher for borosilicate than for soda-lime glass.* Computation of the mean and standard deviation for all rods falling within the fatigue-free region of Figure 2 accordingly gives $\sigma_m P^{1/3} = 137 \pm 8$ MPa N^{1/3} (87 specimens) for soda-lime glass and $\sigma_m P^{1/3} = 173 \pm 19$ MPa N^{1/3} (129 specimens) for borosilicate glass.

Next, the specimens broken in nitrogen were examined optically to obtain the parameter in c_m in Equation (5).⁽²²⁾ For this purpose, surface trace measurements were made of the two indentation flaws which had survived each rod failure. It is argued that the radial cracks perpendicular to the tensile bend axis must have been taken very close to the instability configuration, and accordingly provide a measure of c_m . The radial cracks parallel to the tensile axis should, of course, be unaffected by the bending, and thus

* This compares with the 2–3% error obtainable in the biaxial testing of indented soda-lime glass plates, where specimen alignment difficulties can be effectively eliminated altogether.⁽²⁹⁾ The choice of rods rather than plates in this study is a reflection of our ultimate aim of expanding the test programme to the domain of optical fibres.